Fermionic Atoms in a Three Dimensional Optical Lattice: Observing Fermi Surfaces, Dynamics, and Interactions

Michael Köhl,* Henning Moritz, Thilo Stöferle, Kenneth Günter, and Tilman Esslinger
Institute of Quantum Electronics, ETH Zürich, Hönggerberg, CH-8093 Zürich, Switzerland
(Received 12 October 2004; published 4 March 2005)

We have studied interacting and noninteracting quantum degenerate Fermi gases in a three-dimensional optical lattice. We directly image the Fermi surface of the atoms in the lattice by turning off the optical lattice adiabatically. Because of the confining potential, gradual filling of the lattice transforms the system from a normal state into a band insulator. The dynamics of the transition from a band insulator to a normal state is studied, and the time scale is measured to be an order of magnitude larger than the tunneling time in the lattice. Using a Feshbach resonance, we increase the interaction between atoms in two different spin states and dynamically induce a coupling between the lowest energy bands. We observe a shift of this coupling with respect to the Feshbach resonance in free space which is anticipated for strongly confined atoms.

DOI: 10.1103/PhysRevLett.94.080403 PACS numbers: 03.75.Ss, 05.30.Fk, 34.50.−s, 71.18.+y

The exploration of quantum degenerate gases of fermionic atoms is driven by the ambition to get deeper insight into long-standing problems of quantum many-body physics, such as high temperature superconductivity. Very recently, the crossover regime between a strongly interacting two-component Fermi gas and a molecular Bose-Einstein condensate has been studied in harmonic traps [1–5]. These experiments mark a milestone towards the understanding of superfluidity of fermionic atoms. However, the analogy to an electron gas in a solid is limited since there the electrons experience a periodic lattice potential. The lattice structure is, in fact, a key ingredient for most models describing quantum many-body phenomena in materials. It has been suggested that strongly interacting fermionic atoms in optical lattices could be employed for studies of high-T_c superconductivity [6], Mott-insulating phases [7], Bose condensation of fermionic particle-hole pairs [8], or interacting spin systems [9].

Here we report on an experiment bridging the gap between current ultracold atom systems and fundamental concepts in condensed matter physics. A quantum degenerate Fermi gas of atoms is prepared in the crystal structure of a three-dimensional optical lattice potential created by three crossed standing laser waves. The unique control over all relevant parameters in this system allows us to carry out experiments which are not feasible with solid-state systems.

It was conceived by Jaksch *et al.* that ultracold atoms exposed to the periodic potential of an optical lattice are an almost ideal realization of a Hubbard model [10]. This model is elementary to describe the quantum physics of many electrons in a solid. It takes into account a single band of a static lattice potential and assumes the interactions to be purely local [11]. Ultracold atoms in an optical lattice give a very direct access to the underlying physics. The fundamental parameters include the tunnel coupling between adjacent lattice sites, the atom-atom interactions, and the dimensionality of the system. Previous experiments with far-detuned three-dimensional optical lattices [12–14] were always carried out with bosonic atoms, and experiments with fermions were restricted to a single standing wave [15]. In the latter situation many atoms can reside in each standing wave minimum, but formation of a band insulator is prevented by the weak transverse confinement. The observed inhibition of transport [16] is due to localized states and therefore differs qualitatively from the band insulator which we create in the three-dimensional optical lattice.

The experiments are performed in a modified apparatus previously used to study bosonic rubidium atoms in optical lattices [14,17]. A mixture of bosonic ^{87}Rb and fermionic ^{40}K atoms is captured in a magneto-optical trap. For magnetic trapping we optically pump the potassium atoms into the $|F = 9/2, m_F = 9/2\rangle$ and the rubidium atoms into the $|F = 2, m_F = 2\rangle$ hyperfine ground state, with F being the total angular momentum and m_F the magnetic quantum number. The mixture is evaporatively cooled using microwave radiation to selectively remove the most energetic rubidium atoms from the trap. The potassium cloud is sympathetically cooled by thermal contact with the rubidium atoms [18]. After reaching quantum degeneracy for both species with typically 6×10^5 potassium atoms at a temperature of $T/T_F = 0.32$ ($T_F = 260$ nK is the Fermi temperature of the noninteracting gas), we remove all the rubidium atoms from the trap. The potassium atoms are then transferred from the magnetic trap into a crossed beam optical dipole trap whose laser beams possess a wavelength of $\lambda = 826$ nm and are focused at the position of the Fermi gas to $1/e^2$ radii of 50 μm (x axis) and 70 μm (y axis). The initial trapping frequencies are $\omega_x = 2\pi \times 93$ Hz, $\omega_y = 2\pi \times 154$ Hz, and $\omega_z = 2\pi \times 157$ Hz. When loading the optical trap, we turn off the magnetic confinement in such a way that a variable homogeneous magnetic field remains present. In the optical trap we prepare a spin mixture with $(50 \pm 4)\%$ in each of the $|F = 9/2, m_F = -9/2\rangle$ and $|F = 9/2, m_F = -7/2\rangle$ spin states using a

sequence of two radio-frequency pulses. By lowering the depth of the optical trap on a time scale of 2 s we further evaporatively cool the potassium gas. This is done at a bias magnetic field of $B = 227$ G, which is well above the magnetic Feshbach resonance centered at $B_0 = 202.1$ G [1], and the s-wave scattering length between the two fermionic spin states is $a = 118a_0$ (a_0 is the Bohr radius). At the end of the evaporation we reach temperatures between $T/T_F = 0.2$ and 0.25 with 5×10^4 to 2×10^5 particles, respectively.

Prior to loading the atoms into the optical lattice we tune the magnetic field to $B = (210 \pm 0.1)$ G, such that the s-wave scattering length between the two states vanishes. Then the standing wave laser field along the vertical z axis is turned on. Subsequently, the optical dipole trap along the y axis is turned off and a standing wave laser field along the same axis is turned on, followed by the same procedure along the x axis. In order to keep the loading of the atoms into the lattice as adiabatic as possible the intensities of the lasers are slowly increased (decreased) using exponential ramps with time constants of 10 ms (25 ms) and durations of 20 ms (50 ms), respectively.

In its final configuration the optical lattice is formed by three orthogonal standing waves with mutually orthogonal polarizations and $1/e^2$ radii of 50 μm (x axis) and 70 μm (y axis and z axis), which are derived from the same lasers as for the optical dipole trap. The laser fields of the three beams have a linewidth of the order of 10 kHz and their frequencies are offset with respect to each other by between 15 and 150 MHz. The resulting optical potential depth $V_{x,y,z}$ is proportional to the laser intensity and is conveniently expressed in terms of the recoil energy $E_r = \hbar^2 k^2/(2m)$, with $k = 2\pi/\lambda$ and m being the atomic mass. The lattice depth was calibrated by modulating the laser intensity and studying the parametric heating. The calibration error is estimated to be $<10\%$.

The potential created by the optical lattice results in a simple cubic crystal structure and the Gaussian intensity profiles of the lattice beams give rise to an additional confining potential which varies with the laser intensity. As a result, the sharp edges characterizing the $T = 0$ distribution function for the quasimomentum in the homogeneous case [19] are expected to be rounded off. A quantitative picture can be obtained by considering a tight-binding Hamiltonian to describe noninteracting fermions in an optical lattice with an additional harmonic confinement [20]. At $T = 0$ the inhomogeneous system is characterized by the total atom number N and by the characteristic length ζ over which the potential shift due to the harmonic confinement equals the tunnel coupling matrix element J. One finds $\zeta_\alpha = \sqrt{2J/m\omega_\alpha^2}$, with the frequencies of the external harmonic confinement given by ω_α ($\alpha = x, y, z$). The density distribution scaled by ζ_α and the momentum distribution of the atoms in the lattice depend only on the characteristic density $\rho_c = \frac{Nd^3}{\zeta_x\zeta_y\zeta_z}$, where d is the lattice spacing [7]. For a three-dimensional lattice with $20 \times 20 \times 20$ sites we have numerically calculated the characteristic density for the onset of a band insulator to be $\rho_c \simeq 60$. For this value of ρ_c the occupation number at the center of the trap is larger than 0.99. It has been pointed out that a fermionic band insulator in an optical lattice with confining potential constitutes a high fidelity quantum register [21].

In the experiment we probe the population within the first Brillouin zones by ramping down the optical lattice slowly enough for the atoms to stay adiabatically in the lowest band while quasimomentum is approximately conserved [22]. We lower the lattice potential to zero over a time scale of 1 ms. After 1 ms we switch off the homogeneous magnetic field and allow for a total of 9 ms of ballistic expansion before we take an absorption image of the expanded atom cloud. The momentum distribution obtained from these time of flight images, shown in Fig. 1, reproduces the quasimomentum distributions of the atoms inside the lattice. With increasing characteristic density the initially circular shape of the Fermi surface develops extensions pointing towards the Bragg planes and finally transforms into a square shape completely filling the first Brillouin zone deeply in the band insulator. We have observed population of higher bands if more atoms are filled into the lattice initially. In Fig. 2 the experimental data for momentum distributions along the line with quasimomentum $q_y = 0$ are compared to the results of numerical simulations using the same characteristic densities.

When imaging the cloud along the x direction we find a homogeneous filling of the band in the vertical (z) direction, probably due to the change in the harmonic confinement while loading the lattice combined with the presence of gravity. This asymmetry between the horizontal x, y, and the vertical z directions vanishes when the gas approaches the band insulating regime. We have examined the level of adiabaticity of our loading scheme into the optical lattice by transferring the atoms from the band insulator back into the crossed beam dipole trap. There we find a temperature of $0.35T_F$ when the initial temperature prior to loading into the lattice was $0.2T_F$.

We have studied the dynamic response of the noninteracting Fermi gas to a change in the characteristic density

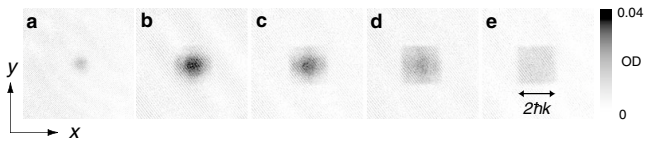

FIG. 1. Observing the Fermi surface. Time of flight images obtained after adiabatically ramping down the optical lattice. The characteristic density increases from left to right. (a) Image of 3500 atoms per spin state and a potential depth of the optical lattice of $5E_r$. Images (b)–(e) were obtained with 15 000 atoms per spin state. The potential depths of the optical lattices were (b) $5E_r$, (c) $6E_r$, (d) $8E_r$, and (e) $12E_r$. The images show the optical density (OD) integrated along the vertically oriented z axis after 9 ms of ballistic expansion.

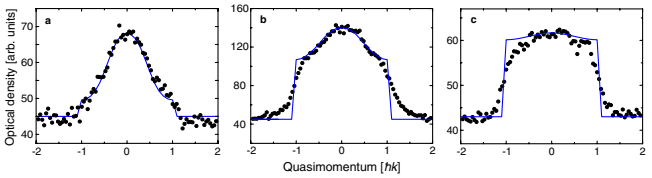

FIG. 2 (color online). Analysis of the density distributions. The dots are cuts through the measured density distribution for quasimomentum $q_y = 0$ after adiabatically ramping down the optical lattice. (a) Normal state with $\rho_c = 14.5$, (b) band insulator with $\rho_c = 137$, and (c) band insulator with $\rho_c = 2500$. We have numerically calculated the momentum distribution function of fermions in the lowest band of a three-dimensional lattice with $20 \times 20 \times 20$ sites and characteristic lengths $\zeta_x/d = 3.2$, $\zeta_y/d = 2.6$, $\zeta_z/d = 2.5$ [(a),(b)] and $\zeta_x/d = 1$, $\zeta_y/d = 0.8$, $\zeta_z/d = 0.8$ (c), assuming zero temperature (solid lines). Experimental data of (c) are averaged over five images. Imperfect adiabaticity during the switch-off of the optical lattice may cause the rounding off of the experimental data at the edge of the Brillouin zone in (b) and (c). The calculated momentum distribution function is scaled to match the experimental data using identical scale factors for all graphs.

from a value deep in the band insulating regime to a value below. In the latter regime the fermions are delocalized over several sites of the optical lattice and an interference pattern is observed when the atoms are abruptly released from the lattice. The width of the interference peaks is a measure of the length scale over which the atoms are delocalized in the lattice or, equivalently, their coherence length. We change the characteristic density *in situ* by varying the strength of the lattice laser beams. Starting from an initial characteristic density of $\rho_c = 16$ in an optical lattice with a potential depth of $5E_r$ we create a band insulator with a characteristic density of $\rho_c = 2700$ at a potential depth of $15E_r$. After holding the atoms for 5 ms we reduce the potential depth back to $5E_r$, using an exponential ramp with duration and time constant t_r. This is followed by a rapid switch-off of the lattice [see Fig. 3(a)]. We measure the width of the central momentum peak in the time of flight images for different durations t_r and obtain the time scales $\tau_x = (2.7 \pm 0.4)$ ms and $\tau_y = (3.8 \pm 0.3)$ ms in the x and the y directions, respectively. This corresponds to approximately 10 times the time scale for tunneling given by $h/2zJ$ at a potential depth of $5E_r$, where z is the coordination number of the lattice. This nontrivial dynamics appears to be significantly slower than the time scale measured for the transition of a Mott-insulating state to a superfluid state using bosonic atoms in an optical lattice [13]. The comparatively slow dynamics of delocalization of the fermions when approaching the normal state is most likely due to Pauli blocking which prevents tunneling of atoms in regions where the lowest band is full and the atoms are well localized.

We investigate the interacting regime in the lattice starting from a noninteracting gas deep in a band insulator with $V_x = 12E_r$ and $V_y = V_z = 18E_r$, and corresponding trapping frequencies of $\omega_x = 2\pi \times 50$ kHz and $\omega_y = \omega_z = 2\pi \times 62$ kHz in the individual minima. A short radio-frequency pulse is applied to transfer all atoms from the $|F = 9/2, m_F = -7/2\rangle$ state into the $|F = 9/2, m_F = -5/2\rangle$ state, with the atoms in the $|F = 9/2, m_F = -9/2\rangle$ state remaining unaffected. We ramp the magnetic field with an inverse sweep rate of 12 μs/G to different final values around the Feshbach resonance [see Fig. 4(a)] located at $B = 224$ G [23]. The sweep across the Feshbach resonance goes from the side of repulsive interactions towards the side of attractive interactions. When using this direction of the sweep there is no adiabatic conversion to molecules. After turning off the optical lattice adiabatically and switching off the magnetic field, we measure the momentum distribution. To see the effect of the interactions we determine the fraction of atoms transferred into higher bands. For final magnetic field values well above the Feshbach resonance we observe a significant increase in the number of atoms in higher bands along the weak axis of the lattice, demonstrating an interaction-induced coupling between the lowest bands. Since the s-wave interaction is changed on a time scale short compared to the tunneling

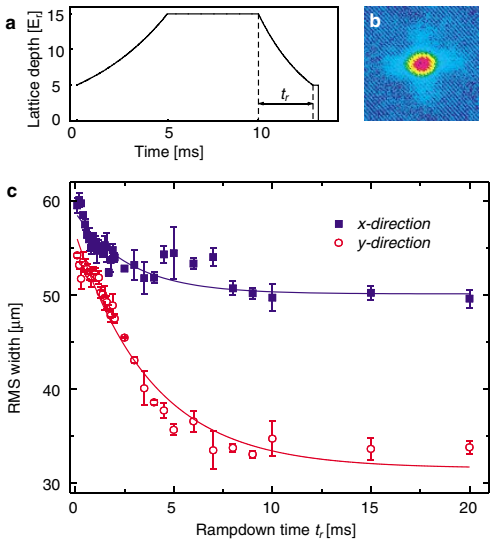

FIG. 3 (color online). Restoring phase coherence. (a) Control sequence for the depth of the optical lattice. (b) Pseudocolor image of the momentum distribution after releasing the atoms from the initial optical lattice of $5E_r$ and 6 ms ballistic expansion. It reveals the central momentum peak and the matter wave interference peaks at $\pm 2\hbar k$. The data are averaged over five repetitive measurements. (c) Width of the central momentum peak obtained from Gaussian fits to the atomic density distribution. The initial width is determined by the momentum spread of an atom localized in the vibrational ground state of a lattice well. The 10% difference in this size comes from slightly different magnifications of the imaging system in the two orthogonal directions. The difference in the asymptotic values of the width can most likely be attributed to the loading sequence of the lattice and to the asymmetry of the confining potentials due to the different beam waists. The error bars show the statistical error of four repetitive measurements.

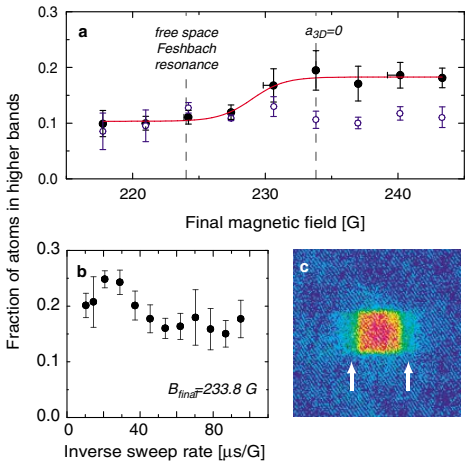

FIG. 4 (color online). Interaction-induced transition between Bloch bands. (a) Transferring fermions into higher bands using a sweep across the Feshbach resonance (filled symbols). The inverse magnetic field sweep rate is 12 μs/G. The line shows a sigmoidal fit to the data. The open symbols show a repetition of the experiment with the atoms prepared in the spin states $|F = 9/2, m_F = -9/2\rangle$ and $|F = 9/2, m_F = -7/2\rangle$ where the scattering length is not sensitive to the magnetic field. The magnetic field is calibrated by rf spectroscopy between Zeeman levels. Because of the rapid ramp, the field lags behind its asymptotic value and the horizontal error bars represent this deviation. (b) Fraction of atoms in higher bands for a final magnetic field of 233 G for different magnetic field sweep rates. The vertical error bars show the statistical error of four repetitive measurements. (c) Momentum distribution for a final magnetic field of $B = 233$ G and a 12 μs/G sweep rate. Arrows indicate the atoms in the higher bands.

time between adjacent potential minima we may regard the band insulator as an array of harmonic potential wells. It has been shown that increasing the s-wave scattering length for two particles in a harmonic oscillator shifts the energy of the two-particle state upwards until the next oscillator level is reached [24]. In our case this leads to a population of higher energy bands. The fraction of atoms transferred could be limited by the number of doubly occupied lattice sites and tunneling in the higher bands. The number of doubly occupied sites could be measured by studying the formation of molecules in the lattice. In addition, we observe a shift of the position of the Feshbach resonance from its value in free space to larger values of the magnetic field [see Fig. 4(a)], which has been predicted for tightly confined atoms in an optical lattice [25]. This mechanism for a confinement induced resonance is related to the phenomenon predicted for one-dimensional quantum gases [26] which has as yet escaped experimental observation. For a quantitative description of this strongly interacting Fermi gas on a lattice a multiband Hubbard model could be considered, but these are even in the static case notoriously difficult or even impossible to solve with the present methods [27].

In conclusion, we have created a fermionic many-particle quantum system on a lattice. We have demonstrated the dynamic control over the parameters of the system such as filling and interactions which is not feasible in solid-state systems. For the noninteracting static regime we find good agreement between our measurements and a theoretical model. Both the dynamic measurements and the strongly interacting case pose challenges for the present theoretical understanding of many-particle fermionic systems on optical lattices.

We thank G. Blatter, C. Bruder, H. P. Büchler, S. Jonsell, A. Muramatsu, M. Rigol, C. Schori, P. Törmä, and M. Troyer for insightful discussions, and SNF, SEP Information Sciences, and QSIT for funding.

*Electronic address:Koehl@phys.ethz.ch

[1] C. A. Regal, M. Greiner, and D. S. Jin, Phys. Rev. Lett. **92**, 040403 (2004).
[2] M. Bartenstein *et al.*, Phys. Rev. Lett. **92**, 120401 (2004).
[3] M. W. Zwierlein *et al.*, Phys. Rev. Lett. **92**, 120403 (2004).
[4] J. Kinast *et al.*, Phys. Rev. Lett. **92**, 150402 (2004).
[5] T. Bourdel *et al.*, Phys. Rev. Lett. **93**, 050401 (2004).
[6] W. Hofstetter, J. I. Cirac, P. Zoller, E. Demler, and M. D. Lukin, Phys. Rev. Lett. **89**, 220407 (2002).
[7] M. Rigol, A. Muramatsu, G. G. Batrouni, and R. T. Scalettar, Phys. Rev. Lett. **91**, 130403 (2003).
[8] C. Lee, Phys. Rev. Lett. **93**, 120406 (2004).
[9] L. Santos *et al.*, Phys. Rev. Lett. **93**, 030601 (2004).
[10] D. Jaksch, C. Bruder, J. I. Cirac, C. W. Gardiner, and P. Zoller, Phys. Rev. Lett. **81**, 3108 (1998).
[11] J. Hubbard, Proc. R. Soc. London A **276**, 238 (1963).
[12] M. T. DePue, C. McCormick, S. L. Winoto, S. Oliver, and D. S. Weiss, Phys. Rev. Lett. **82**, 2262 (1999).
[13] M. Greiner, O. Mandel, T. Esslinger, T. W. Hänsch, and I. Bloch, Nature (London) **415**, 39 (2002).
[14] T. Stöferle, H. Moritz, C. Schori, M. Köhl, and T. Esslinger, Phys. Rev. Lett. **92**, 130403 (2004).
[15] G. Modugno, F. Ferlaino, R. Heidemann, G. Roati, and M. Inguscio, Phys. Rev. A **68**, 011601(R) (2003).
[16] L. Pezze *et al.*, Phys. Rev. Lett. **93**, 120401 (2004).
[17] H. Moritz, T. Stöferle, M. Köhl, and T. Esslinger, Phys. Rev. Lett. **91**, 250402 (2003).
[18] G. Modugno *et al.*, Science **297**, 2240 (2002).
[19] N. W. Ashcroft and N. D. Mermin, *Solid States Physics* (Saunders College Publishing, Philadelphia, PA, 1976).
[20] M. Rigol and A. Muramatsu, Phys. Rev. A **69**, 053612 (2004).
[21] L. Viverit, C. Menotti, T. Calarco, and A. Smerzi, Phys. Rev. Lett. **93**, 110401 (2004).
[22] M. Greiner, I. Bloch, O. Mandel, T. W. Hänsch, and T. Esslinger, Phys. Rev. Lett. **87**, 160405 (2001).
[23] C. A. Regal and D. S. Jin, Phys. Rev. Lett. **90**, 230404 (2003).
[24] T. Busch, B.-G. Englert, K. Rzazewski, and M. Wilkens, Found. Phys. **28**, 549 (1998).
[25] P. O. Fedichev, M. J. Bijlsma, and P. Zoller, Phys. Rev. Lett. **92**, 080401 (2004).
[26] M. Olshanii, Phys. Rev. Lett. **81**, 938 (1998).
[27] M. Troyer and U. Wiese, cond-mat/0408370.